

# The cardiac $\text{Na}^+/\text{K}^+$ ATPase: An updated, thermodynamically consistent model

Michael Pan<sup>1</sup>, Peter J. Gawthrop<sup>1</sup>, Joseph Cursons<sup>2</sup>, Kenneth Tran<sup>3</sup>,  
and Edmund J. Crampin<sup>1,4,5</sup>

<sup>1</sup>Systems Biology Laboratory, School of Mathematics and Statistics, and Department of Biomedical Engineering, Melbourne School of Engineering, University of Melbourne, Parkville, Victoria 3010, Australia.

<sup>2</sup>Bioinformatics Division, Walter and Eliza Hall Institute of Medical Research, Parkville, Victoria 3052, Australia.

<sup>3</sup>Auckland Bioengineering Institute, University of Auckland, Auckland, New Zealand

<sup>4</sup>ARC Centre of Excellence in Convergent Bio-Nano Science and Technology, Melbourne School of Engineering, University of Melbourne, Parkville, Victoria 3010, Australia.

<sup>5</sup>School of Medicine, University of Melbourne, Parkville, Victoria 3010, Australia

## Abstract

The  $\text{Na}^+/\text{K}^+$  ATPase is an essential component of cardiac electrophysiology, maintaining physiological  $\text{Na}^+$  and  $\text{K}^+$  concentrations over successive heart beats. [Terkildsen et al. \(2007\)](#) developed a model of the ventricular myocyte  $\text{Na}^+/\text{K}^+$  ATPase to study extracellular potassium accumulation during ischaemia, demonstrating the ability to recapitulate a wide range of experimental data, but unfortunately there was no archived code associated with the original manuscript. Here we detail an updated version of the model and provide CellML and MATLAB code to ensure reproducibility and reusability. We note some errors within the original formulation which have been corrected to ensure that the model is thermodynamically consistent, and although this required some reparameterisation, the resulting model still provides a good fit to experimental measurements that demonstrate the dependence of  $\text{Na}^+/\text{K}^+$  ATPase pumping rate upon membrane voltage and metabolite concentrations. To demonstrate thermodynamic consistency we also developed a bond graph version of the model. We hope that these models will be useful for community efforts to assemble a whole-cell cardiomyocyte model which facilitates the investigation of cellular energetics.

## 1 Introduction

Cardiomyocytes maintain  $\text{Na}^+$  and  $\text{K}^+$  ions within their physiological concentration range, in part by using  $\text{Na}^+/\text{K}^+$  ATPases located on their plasma membranes. The  $\text{Na}^+/\text{K}^+$  ATPase is an electrogenic ion pump that uses energy from ATP hydrolysis to drive the transport of  $\text{Na}^+$  and  $\text{K}^+$  ions against an electrochemical gradient. A previous model of the cardiomyocyte  $\text{Na}^+/\text{K}^+$  ATPase was developed by [Terkildsen et al. \(2007\)](#) and subsequently incorporated into a whole-cell cardiomyocyte model to demonstrate that reduced  $\text{Na}^+/\text{K}^+$  ATPase activity plays a dominant role in extracellular potassium accumulation during ischaemia ([Terkildsen et al., 2007](#); [Terkildsen, 2006](#)). In this manuscript the  $\text{Na}^+/\text{K}^+$  ATPase model of [Terkildsen et al. \(2007\)](#) will subsequently be referred to as the *Terkildsen et al.* model.

The  $\text{Na}^+/\text{K}^+$  ATPase model presented in [Terkildsen et al. \(2007\)](#) was based upon an earlier implementation which proposed thermodynamic constraints and a lumping scheme for model simplification ([Smith and Crampin, 2004](#)). A key development was that the *Terkildsen et al.* model could reproduce a wider range of data which captured the

dependence of the pump current upon membrane voltage (Nakao and Gadsby, 1989), extracellular sodium (Nakao and Gadsby, 1989), intracellular sodium (Hansen et al., 2002), extracellular potassium (Nakao and Gadsby, 1989) and MgATP (Friedrich et al., 1996). Unfortunately the cycling velocity figures presented within the original paper are not reproducible using information supplied in the figure legends (Terkildsen et al., 2007, Fig. 2) and code used to generate those figures was not publicly archived. These issues are exacerbated by apparent errors within the reported equations and parameter values (further described in Section 2) which result in physical and thermodynamic inconsistencies.

Here we address these issues, updating the model to ensure that it is thermodynamically consistent, and archiving MATLAB and CellML (Lloyd et al., 2004) code for reproducibility. This required the modification of several equations (Section 2) and re-parameterisation through fitting to the original data (Section 3). To verify the physical plausibility of the updated model we have also developed a bond graph version (Oster et al., 1971; Gawthrop and Crampin, 2014), and we refer readers to Gawthrop and Smith (1996); Borutzky (2010); and Gawthrop and Bevan (2007) for further information on bond graph theory. Given the thermodynamic consistency of our updated model we believe that it is particularly well-suited for incorporation into community efforts for developing a thermodynamic model of a cardiomyocyte to ultimately study whole-heart cardiac energetics.

## 2 Modifications

The Terkildsen *et al.* model uses the Post-Albers cycle (Apell, 1989), a model in which sodium and potassium ions bind individually on one side of the membrane, and unbind on the other side (Figure 1). The full Post-Albers cycle was simplified to reduce computational complexity by assuming that faster reactions are in rapid equilibrium, reducing the full 15-state model to a four-state model with eight modified rate constants (Smith and Crampin, 2004). The entire cycle was then assumed to be in steady-state such that the model simplified to a single equation for cycling velocity, with metabolite dependence incorporated in a manner that accounted for thermodynamic constraints. We identified three issues while reimplementing the Terkildsen *et al.* model, and made several modifications to remedy these issues:

**Issue 1:** Equilibrium constants were inconsistent with the number of binding sites. For identical binding sites the kinetic rate constants are typically assumed to be proportional to the number of sites available for binding/unbinding (Keener and Sneyd, 2009) and we modified the reaction scheme from Terkildsen et al. (2007) to achieve this (*red parameters within Figure 1*).

**Issue 2:** The detailed balance constraint used during fitting procedure appears to have used an incorrect parameter value with important consequences on the thermodynamic consistency of the model. This constraint relates the kinetic constants defined in Figure 1:

$$\frac{k_1^+ k_2^+ k_3^+ k_4^+ K_{d,Na_e}^0 (K_{d,Na_e})^2 (K_{d,K_i})^2}{k_1^- k_2^- k_3^- k_4^- K_{d,Na_i}^0 (K_{d,Na_i})^2 (K_{d,K_e})^2 K_{d,MgATP}} = \exp\left(-\frac{\Delta G_{MgATP}^0}{RT}\right) \quad (1)$$

where  $R = 8.314$  J/mol/K is the universal gas constant,  $T$  is the absolute temperature, and  $\Delta G_{MgATP}^0$  is the standard free energy of MgATP hydrolysis at pH 0. It appears

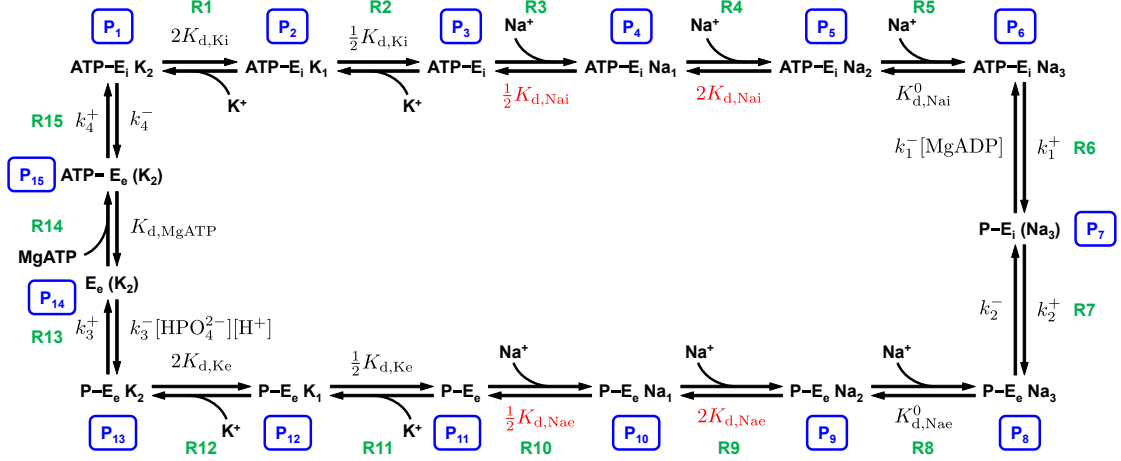


**Figure 1: Reaction scheme of the cardiac  $\text{Na}^+/\text{K}^+$  ATPase model.** Numbers for each pump state (*blue boxes*) and reaction names (*green*) are labelled, with corrected parameters shown in red.

that [Terkildsen et al. \(2007\)](#) started with a standard free energy of  $-29.6\text{kJ/mol}$  at pH 7, but adjusted to a physiological pH rather than pH 0. As a result, substituting the model parameter values into equation (1) results in  $\Delta G_{\text{MgATP}}^0 = -30.2\text{kJ/mol}$ , which is inconsistent with the typical standard free energy of  $11.9\text{kJ/mol}$  at 311K ([Tran et al., 2009](#); [Guynn and Veech, 1973](#)). At a temperature of 310K this results in an overall equilibrium constant over  $10^7$ -fold greater than the correct value. Thus we use  $\Delta G_{\text{MgATP}}^0 = 11.9\text{kJ/mol}$  within the detailed balance constraint.

**Issue 3:** The lumping scheme used to reduce the 15-state model to a 4-state model with modified kinetic constants was similar to [Smith and Crampin \(2004\)](#), however with the updated assignment of electrical dependence in [Terkildsen et al. \(2007\)](#) some expressions were not applicable. As a result, expressions for several modified rate constants ( $\alpha_1^+$ ,  $\alpha_3^+$ ,  $\alpha_2^-$  and  $\alpha_4^-$ ) were incorrect, leading to inaccurate representations of pump kinetics. We have corrected the equations for these modified rate constants:

$$\alpha_1^+ = \frac{k_1^+ \tilde{\text{N}}a_{i,1} \tilde{\text{N}}a_{i,2}^2}{\tilde{\text{N}}a_{i,1} \tilde{\text{N}}a_{i,2}^2 + (1 + \tilde{\text{N}}a_{i,2})^2 + (1 + \tilde{\text{K}}_i)^2 - 1} \quad (2)$$

$$\alpha_3^+ = \frac{k_3^+ \tilde{\text{K}}_e^2}{\tilde{\text{N}}a_{e,1} \tilde{\text{N}}a_{e,2}^2 + (1 + \tilde{\text{N}}a_{e,2})^2 + (1 + \tilde{\text{K}}_e)^2 - 1} \quad (3)$$

$$\alpha_2^- = \frac{k_2^- \tilde{\text{N}}a_{e,1} \tilde{\text{N}}a_{e,2}^2}{\tilde{\text{N}}a_{e,1} \tilde{\text{N}}a_{e,2}^2 + (1 + \tilde{\text{N}}a_{e,2})^2 + (1 + \tilde{\text{K}}_e)^2 - 1} \quad (4)$$

$$\alpha_4^- = \frac{k_4^- \tilde{\text{K}}_i^2}{\tilde{\text{N}}a_{i,1} \tilde{\text{N}}a_{i,2}^2 + (1 + \tilde{\text{N}}a_{i,2})^2 + (1 + \tilde{\text{K}}_i)^2 - 1} \quad (5)$$

where

$$\tilde{N}a_{i,1} = \frac{[Na^+]_i}{K_{d,Na_i}^0 e^{\Delta FV/RT}} \quad \tilde{N}a_{i,2} = \frac{[Na^+]_i}{K_{d,Na_i}} \quad (6)$$

$$\tilde{N}a_{e,1} = \frac{[Na^+]_e}{K_{d,Na_e}^0 e^{(1+\Delta)zFV/RT}} \quad \tilde{N}a_{e,2} = \frac{[Na^+]_e}{K_{d,Na_e}} \quad (7)$$

$$\tilde{K}_i = \frac{[K^+]_i}{K_{d,K_i}} \quad \tilde{K}_e = \frac{[K^+]_e}{K_{d,K_e}} \quad (8)$$

and  $\Delta$  is the unit of charge translocated by the final sodium binding reaction R5. We derive an expression for  $\alpha_1^+$ , and expressions for the other modified rate constants follow similarly. Since the pump states 1 to 6 are lumped together, the constant  $k_1^+$  is scaled according to the ratio between the amount of state 6 and the total amount of states 1–6. If we represent  $x_i$  as the molar amount of state  $i$ , then:

$$\begin{aligned} \alpha_1^+ &= k_1^+ \frac{x_6}{x_6 + x_5 + x_4 + x_3 + x_2 + x_1} \\ &= k_1^+ \frac{1}{1 + x_5/x_6 + x_4/x_6 + x_3/x_6 + x_2/x_6 + x_1/x_6} \\ &= \frac{k_1^+}{1 + 2\tilde{N}a_{i,1}^{-1} + 2\tilde{N}a_{i,1}^{-1}\tilde{N}a_{i,2}^{-1} + \tilde{N}a_{i,1}^{-1}\tilde{N}a_{i,2}^{-2} + 2\tilde{N}a_{i,1}^{-1}\tilde{N}a_{i,2}^{-2}\tilde{K}_i + \tilde{N}a_{i,1}^{-1}\tilde{N}a_{i,2}^{-2}\tilde{K}_i^2} \\ &= \frac{k_1^+ \tilde{N}a_{i,1} \tilde{N}a_{i,2}^2}{\tilde{N}a_{i,1} \tilde{N}a_{i,2}^2 + (1 + \tilde{N}a_{i,2})^2 + (1 + \tilde{K}_i)^2 - 1} \end{aligned} \quad (9)$$

Because it was not possible to fix the above issues without significantly changing the kinetics of the model, we subsequently had to reparameterise the *Terkildsen et al.* model such that it would be physically and thermodynamically consistent. In subsequent sections, we shall refer to the reparameterised model with updated equations as the “updated model” and the model with equations and parameters described in ([Terkildsen et al., 2007](#)) as the “original model”.

### 3 Reparameterisation of the model

Using the updated model’s equations, we fitted parameters to data from *Terkildsen et al.* ([Terkildsen et al., 2007](#); [Terkildsen, 2006](#)). After setting  $\Delta G_{MgATP}^0$  to 11.9kJ/mol in the thermodynamic constraint (Equation (1)), we parameterised the updated model using similar methods to the original model [Terkildsen \(2006\)](#) which minimised an objective function describing divergence of the model from experimental data. Minor changes to the fitting procedure include:

1. The weighting for extracellular potassium above 5.4 mM for the data of [Nakao and Gadsby \(1989\)](#) was increased from  $6\times$  to  $15\times$  to obtain a reasonable fit at physiological concentrations.
2. To ensure that cycling velocity magnitudes matched [Nakao and Gadsby \(1989\)](#), the curve for  $[Na]_e = 150\text{mM}$  was fitted without normalisation.
3. Rather than using a local optimiser with literature sources for initial parameter estimates, we minimised the objective function by using particle swarm optimisation ([Kennedy and Eberhart, 1995](#)) followed by a local optimiser to find a global minimum.

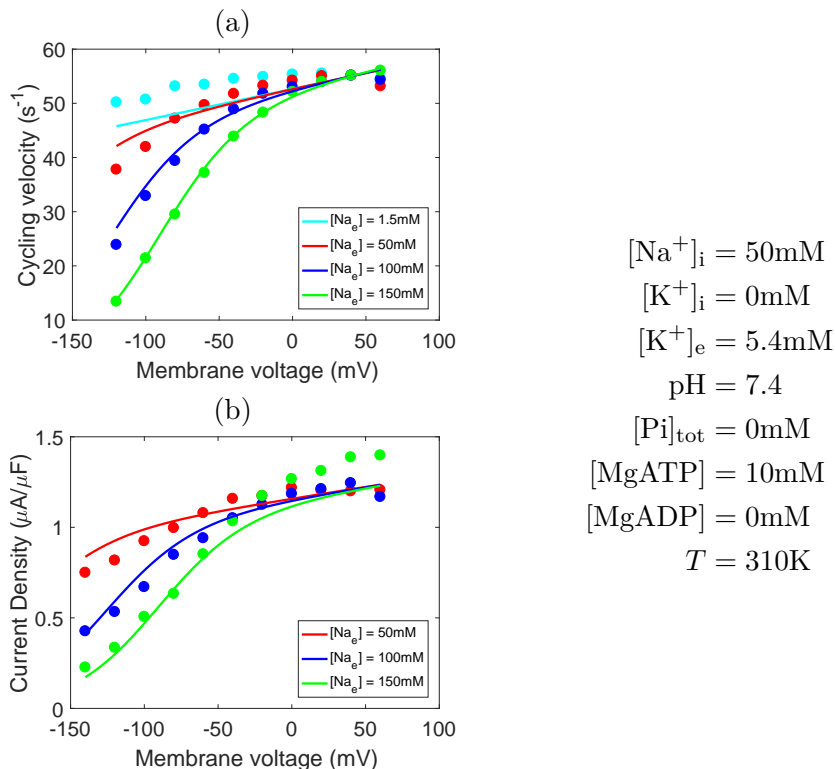


**Figure 2: Model fit of the updated cardiac  $Na^+/K^+$  ATPase model to current-voltage measurements.** (a) Comparison of the model to extracellular sodium and voltage data (Nakao and Gadsby, 1989, Fig. 3), with cycling velocities scaled to a value of  $55s^{-1}$  at  $V = 40mV$ . (b) Comparison of the model to whole-cell current measurements (Nakao and Gadsby, 1989, Fig. 2(a)).

The updated model provides good fits to each data source (Figures 2 & 3), and the quality of fits are comparable to Terkildsen (2006), although we achieved a slightly worse fit at lower extracellular sodium concentrations (Figure 2(a)). It should be noted, however, that our model appears to be more consistent with experimental data that suggest saturated cycling velocity at positive membrane potentials is relatively insensitive to extracellular sodium (Figure 2(b)) (Nakao and Gadsby, 1989). Updated model parameters are given in Table 1 of Appendix A.

The response of the updated model to an action potential input was simulated by using an action potential waveform generated from the Luo and Rudy (2000) model (Faber and Rudy, 2000; Luo and Rudy, 1994) (Figure 4(a)). The original and updated models behave almost identically at resting membrane potentials, but the updated model has a much higher current during the action potential (Figure 4(b)). As noted in Terkildsen (2006), the current of the pump is far lower at physiological intracellular sodium concentrations, thus the pump density needs to be appropriately scaled to be compatible with the Luo-Rudy model. Scaled versions of the  $Na^+/K^+$  ATPase current within the updated and original models are qualitatively similar to that described using the Luo-Rudy equations (Faber and Rudy, 2000; Luo and Rudy, 1994), however there are some differences in the resulting waveforms (Figure 4(c)). In particular, the updated model behaves more similarly to the Luo-Rudy  $Na^+/K^+$  ATPase formulation because it has a more variable

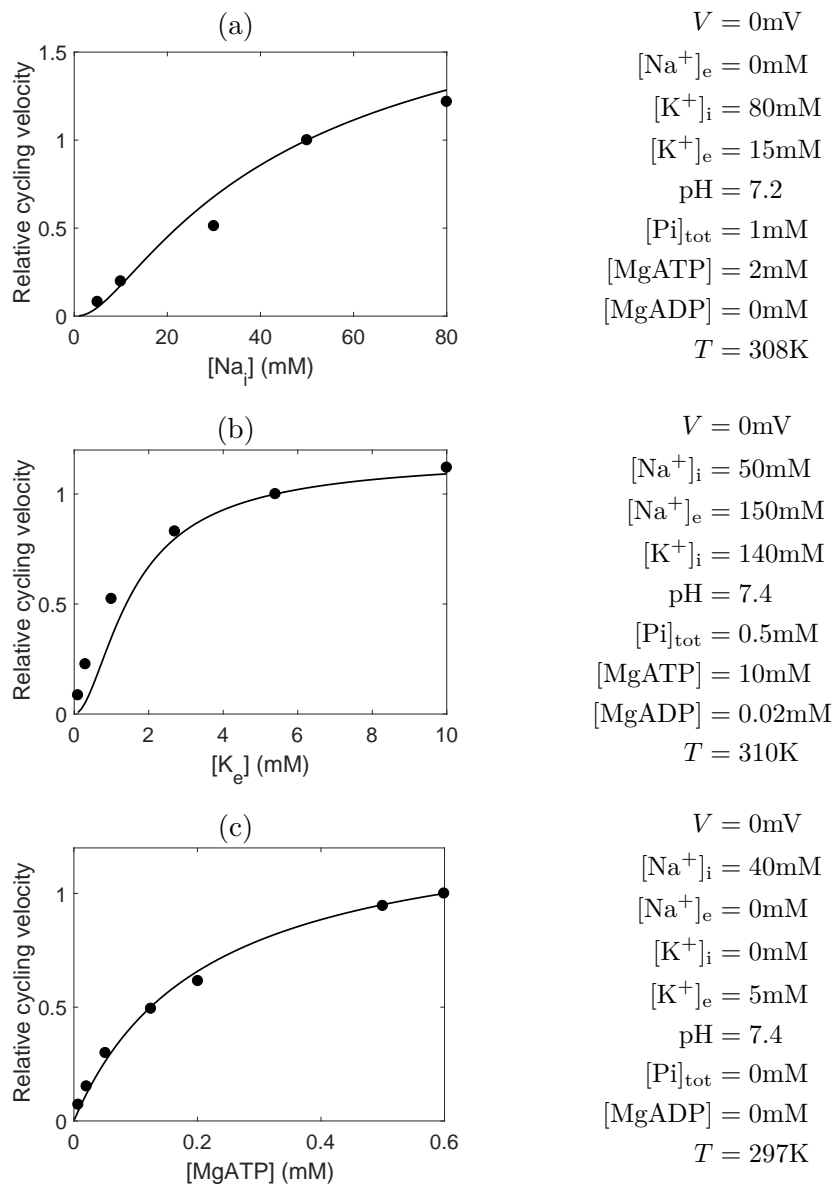


**Figure 3: Model fit of the updated cardiac  $\text{Na}^+/\text{K}^+$  ATPase model to metabolite dependence data.** Simulation conditions are displayed on the right of each figure. (a) Comparison of the model to data with varying intracellular sodium concentrations (Hansen et al., 2002, Fig. 7(a)), normalised to the cycling velocity at  $[\text{Na}]_i = 50\text{mM}$ . (b) Comparison of the model to data with varying extracellular potassium (Nakao and Gadsby, 1989, Fig. 11(a)), normalised to the cycling velocity at  $[\text{K}]_e = 5.4\text{mM}$ . (c) Comparison of the model to data with varying ATP (Friedrich et al., 1996, Fig. 3(b)), normalised to the cycling velocity at  $[\text{MgATP}] = 0.6\text{mM}$ .

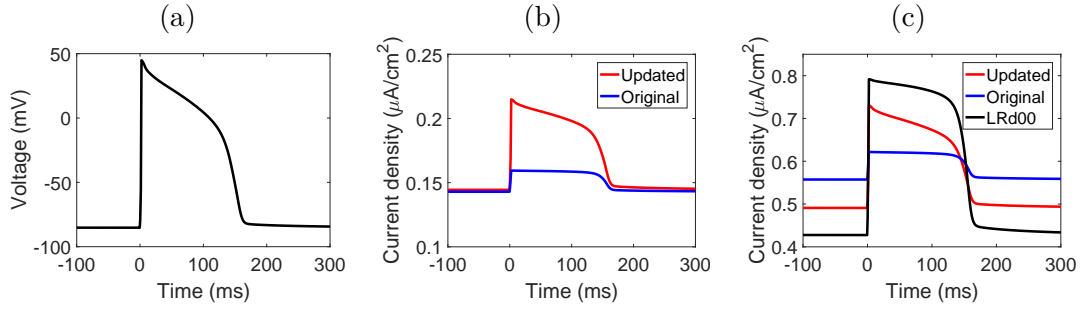


**Figure 4: A comparison of the updated cardiac  $\text{Na}^+/\text{K}^+$  ATPase model to existing models.** (a) The action potential waveform used for pump simulation (Faber and Rudy, 2000); (b) The  $\text{Na}^+/\text{K}^+$  ATPase currents of the original and updated models; (c) A comparison of scaled versions of the updated and original models against the  $\text{Na}^+/\text{K}^+$  ATPase model in Faber and Rudy (2000). The pump density was increased by a factor of 3.4 in the updated model, and by a factor of 3.9 in the original model.  $[\text{Na}^+]_i = 10\text{mM}$ ,  $[\text{Na}^+]_e = 140\text{mM}$ ,  $[\text{K}^+]_i = 145\text{mM}$ ,  $[\text{K}^+]_e = 5.4\text{mM}$ ,  $\text{pH} = 7.095$ ,  $[\text{Pi}]_{\text{tot}} = 0.8\text{mM}$ ,  $[\text{MgATP}] = 6.95\text{mM}$ ,  $[\text{MgADP}] = 0.035\text{mM}$ ,  $T = 310\text{K}$ .

current, and thus we hypothesise that under physiological concentrations, the updated model is more compatible with the whole-cell model by Luo and Rudy. A CellML version of the updated model is included with this manuscript.

## 4 Bond graph model

To verify the physical plausibility of the updated model and to aid incorporation into larger models of cardiac energetics, we have also developed a bond graph version. Bond graphs are an energy-based approach to modelling physical systems, thus they ensure thermodynamic consistency (Gawthrop and Crampin, 2014). The structure of the bond graph model is given in Figure 6 of Appendix B. The process of converting the model into a bond graph required two notable changes to its representation. Firstly, the bond graph model represents the full unsimplified biochemical cycle, and reactions originally assumed to be in rapid equilibrium were replaced by reactions with fast kinetic parameters that conferred the same equilibrium constant. Thus the bond graph model contains 15 states, and is a close but not exact approximation of the kinetic model. Secondly, because kinetic parameters are often thermodynamically inconsistent (Liebermeister et al., 2010), the bond graph approach requires chemical reaction networks to be specified using a different set of parameters: the reaction rate constant  $\kappa$  and species thermodynamic constant  $K$  (Gawthrop and Crampin, 2014). These parameters always describe thermodynamically consistent systems, regardless of their numerical value. As a result, we converted the kinetic parameters of our model into an equivalent set of bond graph parameters (Gawthrop et al., 2015) by using the following matrix equation:

$$\mathbf{Ln}(\mathbf{k}) = \mathbf{M}\mathbf{Ln}(\mathbf{W}\boldsymbol{\lambda}) \quad (10)$$

where  $\mathbf{Ln}$  is the element-wise logarithm operator. The vector  $\mathbf{k}$  contains the kinetic parameters,  $\boldsymbol{\lambda}$  contains the bond graph parameters, and  $\mathbf{M}$  contains stoichiometric

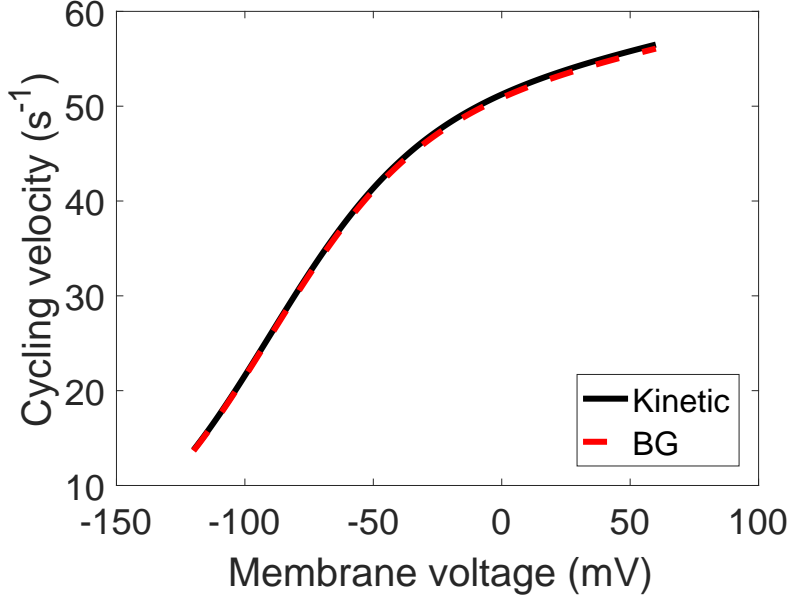


**Figure 5: A comparison of the kinetic and bond graph cardiac  $\text{Na}^+/\text{K}^+$  models.**  $[\text{Na}^+]_i = 50\text{mM}$ ,  $[\text{Na}^+]_e = 150\text{mM}$ ,  $[\text{K}^+]_i = 0\text{mM}$ ,  $[\text{K}^+]_e = 5.4\text{mM}$ ,  $\text{pH} = 7.4$ ,  $[\text{Pi}]_{\text{tot}} = 0\text{mM}$ ,  $[\text{MgATP}] = 10\text{mM}$ ,  $[\text{MgADP}] = 0\text{mM}$ ,  $T = 310\text{K}$ . The bond graph model is formulated using concentration ratios thus zero concentrations were approximated by a concentration of  $0.001\text{mM}$  to avoid numerical errors.

information. The partitions of these matrices are defined as:

$$\mathbf{k} = \begin{bmatrix} k^+ \\ k^- \\ k^c \end{bmatrix}, \quad \mathbf{M} = \begin{bmatrix} I_{n_r \times n_r} & N^f T \\ I_{n_r \times n_r} & N^r T \\ 0 & N^c \end{bmatrix}, \quad \boldsymbol{\lambda} = \begin{bmatrix} \kappa \\ K \end{bmatrix} \quad (11)$$

where

$$k^+ = \text{column vector of forward rate constants} \quad (12)$$

$$k^- = \text{column vector of reverse rate constants} \quad (13)$$

$$\kappa = \text{column vector of reaction rate constants} \quad (14)$$

$$K = \text{column vector of species thermodynamic constants} \quad (15)$$

$$N^f = \text{forward stoichiometric matrix} \quad (16)$$

$$N^r = \text{reverse stoichiometric matrix} \quad (17)$$

The matrices  $k^c$  and  $N^c$  were used to enforce further constraints between the thermodynamic constants of different species, in particular the equilibria of individual ions present within different compartments, and the equilibrium constant of ATP hydrolysis. Assuming that equation (10) can be solved, one possible solution is given by

$$\boldsymbol{\lambda}_0 = \mathbf{W}^{-1} \mathbf{Exp}(\mathbf{M}^\dagger \mathbf{Ln}(\mathbf{k})) \quad (18)$$

where  $\mathbf{Exp}$  is the element-wise exponential operator and  $\mathbf{M}^\dagger$  is the Moore-Penrose pseudo-inverse of  $\mathbf{M}$ . Since the bond graph framework is energy-based, species must be expressed as molar amounts rather than concentrations to adequately compare energies



in different compartments. Therefore we use the diagonal matrix  $\mathbf{W}$  to scale the species thermodynamic constants according to the volume of the compartments they reside in. For consistency with [Terkildsen et al. \(2007\)](#), an intracellular volume of  $W_i = 38\text{pL}$  was used for the species  $\text{Na}_i^+$ ,  $\text{K}_i^+$ ,  $\text{MgATP}$ ,  $\text{MgADP}$ ,  $\text{Pi}$  and  $\text{H}^+$ , an extracellular volume of  $W_e = 5.182\text{pL}$  was used for  $\text{Na}_e^+$ ,  $\text{K}_e^+$ , and a constant of 1 was used for each of the pump states.

The bond graph model was simulated under the conditions described in [Figure 2\(a\)](#) to reproduce the curve for  $[\text{Na}^+]_e = 150\text{mM}$ , using a slowly increasing membrane voltage to induce quasi-steady-state behaviour. There is a high degree of correspondence between the kinetic and bond graph models ([Figure 5](#)). The closeness of the two models suggests that the fast kinetic constants are good approximations of reactions in rapid equilibrium, although we note that the deviation between the bond graph and kinetic models increases slightly at higher cycling velocities when the faster reactions begin to limit flux through the cycle. CellML code describing the bond graph model and reproducing the curve in [Figure 5](#) is provided with this manuscript.

## 5 Conclusion

In this manuscript we describe an updated model for the cardiac  $\text{Na}^+/\text{K}^+$  ATPase model originally developed by [Terkildsen et al. \(2007\)](#). We have corrected errors with the original model formulation and refitted necessary parameters to ensure that the resulting model is thermodynamically consistent while still recapitulating a wide range of experimental data. We note that the updated model has a natural bond graph representation, and include CellML and MATLAB code for both the kinetic and bond graph models to aid reproducibility. We believe that the thermodynamic consistency and improved reusability of our updated model make it ideal for incorporation into future whole-cell models to study cardiac cell energetics.

## 6 Acknowledgements

This research was supported in part by the Australian Government through the Australian Research Council’s Discovery Projects funding scheme (project DP170101358), an Australian Government Research Training Program Scholarship to M.P., and a Research Fellowship (1692) from the Heart Foundation of New Zealand to K.T.

## References

- Apell, H.J., 1989. Electrogenic properties of the Na,K pump. *The Journal of Membrane Biology* 110, 103–114.
- Borutzky, W., 2010. *Bond Graph Methodology*. Springer.
- Faber, G.M., Rudy, Y., 2000. Action Potential and Contractility Changes in  $[\text{Na}^+]_i$  Overloaded Cardiac Myocytes: A Simulation Study. *Biophysical Journal* 78, 2392–2404.
- Friedrich, T., Bamberg, E., Nagel, G., 1996.  $\text{Na}^+,\text{K}^+$ -ATPase pump currents in giant excised patches activated by an ATP concentration jump. *Biophysical Journal* 71, 2486–2500.
- Gawthrop, P., Bevan, G., 2007. Bond-graph modeling. *IEEE Control Systems* 27, 24–45.
- Gawthrop, P., Smith, L., 1996. *Metamodelling: for bond graphs and dynamic systems*. Prentice Hall international series in systems and control engineering, Prentice Hall, London, New York.
- Gawthrop, P.J., Crampin, E.J., 2014. Energy-based analysis of biochemical cycles using bond graphs. *Proceedings of the Royal Society of London A: Mathematical, Physical and Engineering*

- Sciences 470, 20140459.
- Gawthrop, P.J., Cursons, J., Crampin, E.J., 2015. Hierarchical bond graph modelling of biochemical networks. *Proc. R. Soc. A* 471, 20150642.
- Guynn, R.W., Veech, R.L., 1973. The Equilibrium Constants of the Adenosine Triphosphate Hydrolysis and the Adenosine Triphosphate-Citrate Lyase Reactions. *Journal of Biological Chemistry* 248, 6966–6972.
- Hansen, P.S., Buhagiar, K.A., Kong, B.Y., Clarke, R.J., Gray, D.F., Rasmussen, H.H., 2002. Dependence of  $\text{Na}^+$ - $\text{K}^+$  pump current-voltage relationship on intracellular  $\text{Na}^+$ ,  $\text{K}^+$ , and  $\text{Cs}^+$  in rabbit cardiac myocytes. *American Journal of Physiology - Cell Physiology* 283, C1511–C1521.
- Keener, J., Sneyd, J., 2009. *Mathematical Physiology*. volume 8/1 of *Interdisciplinary Applied Mathematics*. Springer New York, New York, NY.
- Kennedy, J., Eberhart, R., 1995. Particle swarm optimization, in: *IEEE International Conference on Neural Networks, 1995. Proceedings*, pp. 1942–1948 vol.4.
- Liebermeister, W., Uhlenhof, J., Klipp, E., 2010. Modular rate laws for enzymatic reactions: thermodynamics, elasticities and implementation. *Bioinformatics* 26, 1528–1534.
- Lloyd, C.M., Halstead, M.D.B., Nielsen, P.F., 2004. CellML: its future, present and past. *Progress in Biophysics and Molecular Biology* 85, 433–450.
- Luo, C.H., Rudy, Y., 1994. A dynamic model of the cardiac ventricular action potential. I. Simulations of ionic currents and concentration changes. *Circulation Research* 74, 1071–1096.
- Nakao, M., Gadsby, D.C., 1989.  $[\text{Na}]$  and  $[\text{K}]$  dependence of the Na/K pump current-voltage relationship in guinea pig ventricular myocytes. *The Journal of General Physiology* 94, 539–565.
- Oster, G., Perelson, A., Katchalsky, A., 1971. Network thermodynamics. *Nature* 234, 393–399.
- Smith, N.P., Crampin, E.J., 2004. Development of models of active ion transport for whole-cell modelling: cardiac sodium–potassium pump as a case study. *Progress in Biophysics and Molecular Biology* 85, 387–405.
- Terkildsen, J., 2006. *Modelling Extracellular Potassium Accumulation in Cardiac Ischaemia*. Masters Thesis. The University of Auckland.
- Terkildsen, J.R., Crampin, E.J., Smith, N.P., 2007. The balance between inactivation and activation of the  $\text{Na}^+$ - $\text{K}^+$  pump underlies the triphasic accumulation of extracellular  $\text{K}^+$  during myocardial ischemia. *American Journal of Physiology - Heart and Circulatory Physiology* 293, H3036–H3045.
- Tran, K., Smith, N.P., Loiselle, D.S., Crampin, E.J., 2009. A Thermodynamic Model of the Cardiac Sarcoplasmic/Endoplasmic  $\text{Ca}^{2+}$  (SERCA) Pump. *Biophysical Journal* 96, 2029–2042.

## A Parameters

**Table 1: Kinetic parameters for the updated cardiac Na<sup>+</sup>/K<sup>+</sup> ATPase model.** Refer to [Figure 1](#) for a schematic.

Parameter	Description	Value
$k_1^+$	Forward rate constant of reaction R6	1423.2 s <sup>-1</sup>
$k_1^-$	Reverse rate constant of reaction R6	225.9048 s <sup>-1</sup>
$k_2^+$	Forward rate constant of reaction R7	11564.8064 s <sup>-1</sup>
$k_2^-$	Reverse rate constant of reaction R7	36355.3201 s <sup>-1</sup>
$k_3^+$	Forward rate constant of reaction R13	194.4506 s <sup>-1</sup>
$k_3^-$	Reverse rate constant of reaction R13	281037.2758 mM <sup>-2</sup> s <sup>-1</sup>
$k_4^+$	Forward rate constant of reaction R15	30629.8836 s <sup>-1</sup>
$k_4^-$	Reverse rate constant of reaction R15	1.574 × 10 <sup>6</sup> s <sup>-1</sup>
$K_{d,Nai}^0$	Voltage-dependent dissociation constant of intracellular Na <sup>+</sup>	579.7295 mM
$K_{d,Nae}^0$	Voltage-dependent dissociation constant of extracellular Na <sup>+</sup>	0.034879 mM
$K_{d,Nai}$	Voltage-independent dissociation constant of intracellular Na <sup>+</sup>	5.6399 mM
$K_{d,Nae}$	Voltage-independent dissociation constant of extracellular Na <sup>+</sup>	10616.9377 mM
$K_{d,Ki}$	Dissociation constant of intracellular K <sup>+</sup>	16794.976 mM
$K_{d,Ke}$	Dissociation constant of extracellular K <sup>+</sup>	1.0817 mM
$K_{d,MgATP}$	Dissociation constant of MgATP	140.3709 mM
$\Delta$	Charge translocated by reaction R5	-0.0550
Pump density	Number of pumps per $\mu\text{m}^2$	1360.2624 $\mu\text{m}^{-2}$

**Table 2: Parameters for the bond graph version of the updated cardiac  $\text{Na}^+/\text{K}^+$  ATPase model.** Parameters were derived by using an intracellular volume of 38pL and an extracellular volume of 5.182pL. Refer to [Figure 6](#) for the bond graph schematic.

Component	Description	Parameter	Value
R1	Reaction R1	$\kappa_1$	330.5462 fmol/s
R2	Reaction R2	$\kappa_2$	132850.9145 fmol/s
R3	Reaction R3	$\kappa_3$	200356.0223 fmol/s
R4	Reaction R4	$\kappa_4$	2238785.3951 fmol/s
R5	Reaction R5	$\kappa_5$	10787.9052 fmol/s
R6	Reaction R6	$\kappa_6$	15.3533 fmol/s
R7	Reaction R7	$\kappa_7$	2.3822 fmol/s
R8	Reaction R8	$\kappa_8$	2.2855 fmol/s
R9	Reaction R9	$\kappa_9$	1540.1349 fmol/s
R10	Reaction R10	$\kappa_{10}$	259461.6507 fmol/s
R11	Reaction R11	$\kappa_{11}$	172042.3334 fmol/s
R12	Reaction R12	$\kappa_{12}$	6646440.3909 fmol/s
R13	Reaction R13	$\kappa_{13}$	597.4136 fmol/s
R14	Reaction R14	$\kappa_{14}$	70.9823 fmol/s
R15	Reaction R15	$\kappa_{15}$	0.015489 fmol/s
P <sub>1</sub>	Pump state ATP–E <sub>i</sub> K <sub>2</sub>	$K_1$	101619537.2009 fmol <sup>-1</sup>
P <sub>2</sub>	Pump state ATP–E <sub>i</sub> K <sub>1</sub>	$K_2$	63209.8623 fmol <sup>-1</sup>
P <sub>3</sub>	Pump state ATP–E <sub>i</sub>	$K_3$	157.2724 fmol <sup>-1</sup>
P <sub>4</sub>	Pump state ATP–E <sub>i</sub> Na <sub>1</sub>	$K_4$	14.0748 fmol <sup>-1</sup>
P <sub>5</sub>	Pump state ATP–E <sub>i</sub> Na <sub>2</sub>	$K_5$	5.0384 fmol <sup>-1</sup>
P <sub>6</sub>	Pump state ATP–E <sub>i</sub> Na <sub>3</sub>	$K_6$	92.6964 fmol <sup>-1</sup>
P <sub>7</sub>	Pump state P–E <sub>i</sub> (Na <sub>3</sub> )	$K_7$	4854.5924 fmol <sup>-1</sup>
P <sub>8</sub>	Pump state P–E <sub>e</sub> Na <sub>3</sub>	$K_8$	15260.9786 fmol <sup>-1</sup>
P <sub>9</sub>	Pump state P–E <sub>e</sub> Na <sub>2</sub>	$K_9$	13787022.8009 fmol <sup>-1</sup>
P <sub>10</sub>	Pump state P–E <sub>e</sub> Na <sub>1</sub>	$K_{10}$	20459.5509 fmol <sup>-1</sup>
P <sub>11</sub>	Pump state P–E <sub>e</sub>	$K_{11}$	121.4456 fmol <sup>-1</sup>
P <sub>12</sub>	Pump state P–E <sub>e</sub> K <sub>1</sub>	$K_{12}$	3.1436 fmol <sup>-1</sup>
P <sub>13</sub>	Pump state P–E <sub>e</sub> K <sub>2</sub>	$K_{13}$	0.32549 fmol <sup>-1</sup>
P <sub>14</sub>	Pump state E <sub>e</sub> (K <sub>2</sub> )	$K_{14}$	156.3283 fmol <sup>-1</sup>
P <sub>15</sub>	Pump state ATP–E <sub>e</sub> (K <sub>2</sub> )	$K_{15}$	1977546.8577 fmol <sup>-1</sup>
K <sub>i</sub>	Intracellular K <sub>i</sub> <sup>+</sup>	$K_{K_i}$	0.0012595 fmol <sup>-1</sup>
K <sub>e</sub>	Extracellular K <sub>e</sub> <sup>+</sup>	$K_{K_e}$	0.009236 fmol <sup>-1</sup>
N <sub>ai</sub>	Intracellular Na <sub>i</sub> <sup>+</sup>	$K_{N_{ai}}$	0.00083514 fmol <sup>-1</sup>
N <sub>ae</sub>	Extracellular Na <sub>e</sub> <sup>+</sup>	$K_{N_{ae}}$	0.0061242 fmol <sup>-1</sup>
MgATP	Intracellular MgATP	$K_{MgATP}$	2.3715 fmol <sup>-1</sup>
MgADP	Intracellular MgADP	$K_{MgADP}$	$7.976 \times 10^{-5}$ fmol <sup>-1</sup>
P <sub>i</sub>	Free inorganic phosphate	$K_{P_i}$	0.04565 fmol <sup>-1</sup>
H	Intracellular H <sup>+</sup>	$K_H$	0.04565 fmol <sup>-1</sup>
mem	Membrane capacitance	$C_m$	153400 fF
zF_5	Charge translocated by R5	$z_5$	-0.0550
zF_8	Charge translocated by R8	$z_8$	-0.9450

## B Bond graph model structure

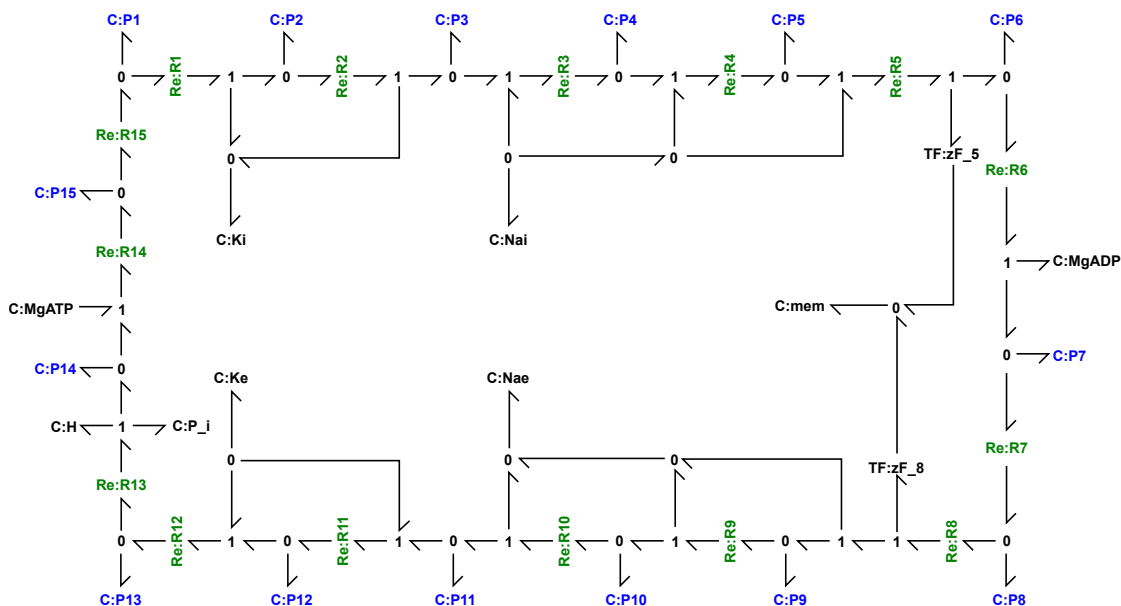


**Figure 6: Bond graph structure of the cardiac  $\text{Na}^+/\text{K}^+$  ATPase model.** Pump states are coloured in blue, and reactions are coloured in green. The names for these components are consistent with their labels in Figure 1.

Notes: This model has been checked for reproducibility. The MATLAB code provided successfully reproduces the Figures 2-5 both qualitatively and quantitatively. Additionally, the SED-ML models provided for each figure also accurately reproduces the reported results, however OpenCOR is unable to display overlaid figures as seen in the paper. It should be noted that no SED-ML or Cell-ML codes were provided for Figure 4. The provided Cell-ML models were annotated using SEMGEN, including the bond graph model.

Specific comments on bond graphs: Bond graphs model the flow of energy throughout networks using pairs of variables whose product is power. The appropriate choice of these pairs for use in chemical reactions networks is chemical potentials ( $\mu$ ) and molar flow rates ( $v$ ). Both of these can be annotated in semgen, however chemical potentials ( $\mu$ ) requires free text descriptions to be added to clarify which reaction they belong to. Additionally the composite annotation of molar flows ( $v$ ) contains customized made terms. It is suggested that the authors either provide a detail description of the biochemical cycle in their paper or reference a source where this can be found. Specifically the reacting species involved at each of the 15 stages of the cycle should be made available to enable further annotation.